Study of Regional Dark Mantle Deposits (RDMDs) at Sinus Aestuum in the central nearside of the Moon using high resolution data from recent lunar missions. Satadru Bhattacharya, Sriram Saran, Prakash Chauhan, Anup Das and Ajai, Space Applications Centre (ISRO), Ahmedabad – 380 015, India (satadru@sac.isro.gov.in).

Introduction: High resolution data from recent lunar missions have been used to study the Regional Dark Mantle Deposits (RDMDs) at Sinus Aestuum in the central nearside of the Moon. RDMDs are referred to as the very low albedo deposits of pyroclastic origin that mantle mare and highland regions [*e.g.*, 1-3]. Spectral analysis based on Chandrayaan-1 Moon Mineralogy Mapper (M^3) data indicates that the dark haloed craters within the RDMDs at the study area show a strong 2000-nm spectral absorption that almost completely lacks a 1000-nm feature suggesting the presence of spinel group of minerals as previously reported by [4]. Western (Sinus Aestuum I) and eastern (Sinus Aestuum II) Sinus Aestuum RDMDs are the only extensive spinel-rich pyroclastic deposits on the Moon [4]. It is therefore important to carry out a detailed compositionnal and morphological analysis of the RDMDs at Sinus Aestuum in order to get insights into the style of formation of such extensive and unusual pyroclastic deposits on the lunar surface. Apart from Chandrayaan-1 M^3 Level 2 (thermally corrected) reflectance data of optical periods OP1B and OP2A, we have also used high resolution LRO Mini-RF data and LROC NAC data in conjunction with LRO LOLA data to study the nature of the pyroclastic deposits and morphology of the sourcevents in the RDMDs that were previously thought to have been buried by younger Sinus Aestuum mare [3].

Methods: A False Color Composite (FCC) mosaic of the study area has been generated using 11 M^3 scenes based on the band ratio technique given by [5]. The central wavelength and band area of 2000-nm spinel absorption feature have been derived following the method given by [6]. LRO Mini-RF backscatter and Circular Polarization Ratio (CPR) images have been obtained to study the nature of the Sinu Aestuum pyroclastics. M-chi decomposition [7] of a small subset of the Mini-RF data over a positive relief feature situated at the southeastern part of Sinus Aestuum has also been carried to unambiguously differentiate the single bounce, double bounce and randomly-polarized backscatter [7] in the study area. LROC NAC images covering southern part of western i.e., Sinus Aestuum I pyroclastic deposits have also been analyzed.

Observations and Discussion: In the M^3 FCC mosaic (Fig. 1), spinel-rich lithologies appear red. A strong 2-μm feature centered at ~2150 nm is evident from Fig. 2. The central wavelength values of 2000-nm spinel feature are consistent with chromites [4]. We have plotted band center of 2000-nm spinel feature against the band area of the spectra collected from Sinus Aestuum RDMDs and spinel spectra from crater Endymion as recently reported by [8] and compared with the band center and band area values of pure terrestrial spinels and chromites (data source – RELAB) based on the data provided by [9]. The 2000-nm band centre values of chromite spectra from Sinus Aestuum RDMDs range from 2067 – 2287 nm, which are consistent with the band center values of terrestrial chormites (Fig. 2). The differences in band area values of Sinus Aestuum chromites and terrestrial chromites could be attributed to the relative purity of chromites in the Sinus Aestuum and terrestrial chromite spectra. Similarly, differences in band area values are also observed in case of Endymion spinel and pure terrestrial spinel, the latter having higher values of band area due to more pure samples. The location of the 2000-nm spinel feature of Endymion spinels occur at relatively shorter wavelength as compared to that of pure terrestrial spinels (Fig. 2), which could be due to the steeper continuum slopes associated with the lunar spinel spectra. Continuum removal of the spinel spectra from crater Endymion pull down the 2000-nm band center values toward the shorter wavelength.

Apart from high spectral resolution M^3 data, two very high resolution LROC NAC scenes (M109338400LC, M109338400RC) have also been analyzed over a small subset of southern part of western i.e., Sinus Aestuum I in search for possible source vents of the pyroclastic deposits at the study area. Multiple low-albedo deposits in the remnant highlands of the southern part of Sinum Aestuum I RDMD deposit are observed in the high resolution LROC NAC images as shown in Figures 4A and 4B. The low-albedo deposits (Figs. 4A and 4B) could possibly be the source vents for the extensive pyroclastic deposits at Sinus Aestuum and are morphologically quite similar to that of the Pele vent on the Galilean satellite Io as observed by [10]. We have also analyzed S-band Mini-RF data from LRO mission over the Sinus Aestuum region to study the extent and distribution of pyroclastic deposits. The RDMDs at Sinus Aestuum are characterized by very low radar backscatter and Circular Polarisation Ratio (CPR) values because of the presence of very fine sub-millimetre sized pyroclastic glass and glass beads. A total backscattered power (S_0) image of a part of the Sinus Aestumm region (Fig. 3A) is overlaid on the LOLA DEM to show the distribution of backscatter values in a 3D spatial conext. We have generated CPR (Fig. 3B) and m-chi decomposition

images (Fig. 3C) for the same region as shown in Figs. 3B and 3C respectively. A vent/fissure like structure has clearly been observed as indicated by arrows in Figures 3A-C. The unsual topography of this vent structure could be explained by a combined analysis of S_0 (Fig. 3A) and CPR (Fig. 3B) images as they are oppositely afftected by the topography. Many such possible vents were detected by the combined analysis of radar and DEM datasets in the Sinus Aestumm region.

Conclusions: Chromium-spinel bearing dark haloed craters within the pyroclastic deposits of Sinus Aestuum have been characterized based on band ratioing techniques and spectral band parameters, namely, band center and band area. Very high resolution LROC NAC and LRO Mini-RF data have been analyzed and numerous non-circular vents have been identified and mapped in the southern and southeastern parts of Sinus Aestuum I and II RDMDs respectively that were previously thought to have been buried. Morphology of the source vents are similar to the low-albedo deposit from the plume generated by the Pele vent on Galilean satellite Io as described by [10]. From the present study, it can therefore be concluded that many small eruptions from multiple vents, as seen in remnant highlands of southern part of Sinun Aestuum I, produced spatially overlapped localized deposits rather than one or two large eruptions from buried central vent as previously proposed by [3].

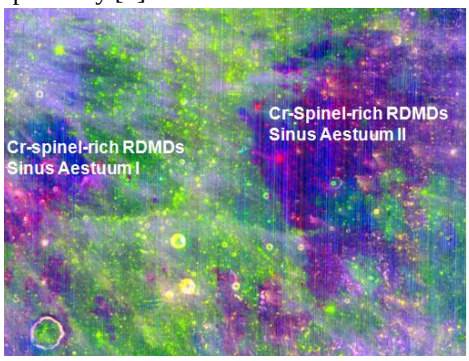

Fig. 1. FCC (R: 1209/1818 nm, G: 730/930 nm, B: 1000/1250 nm) mosaic of Sinus Aestuum highlighting spinel-rich lithologies in red, mafic silicates in green to yellow and pyroclatic deposits in deep blue.

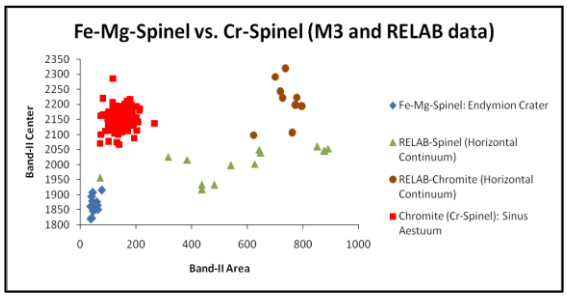

Fig. 2. Band-II center vs. band area plot of chromites and spinels from Sinus Aestuum, Endymion crater and terrestrial chromites and spinels.

Fig. 3.A. Part of an S-band Mini-RF total backscatterd

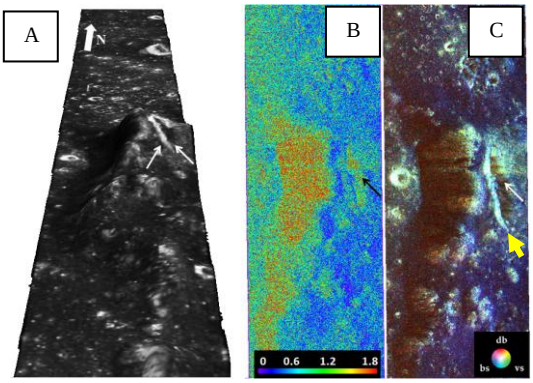

power (S_0) image of a positive relief feature at southeastern part of Sinus Aestuum RDMD draped on LOLA DEM showing a non-circular depression, a possible fissure/volcanic vent (approx. location – 1.87° N; 350.4°E) as indicated by red arrows.

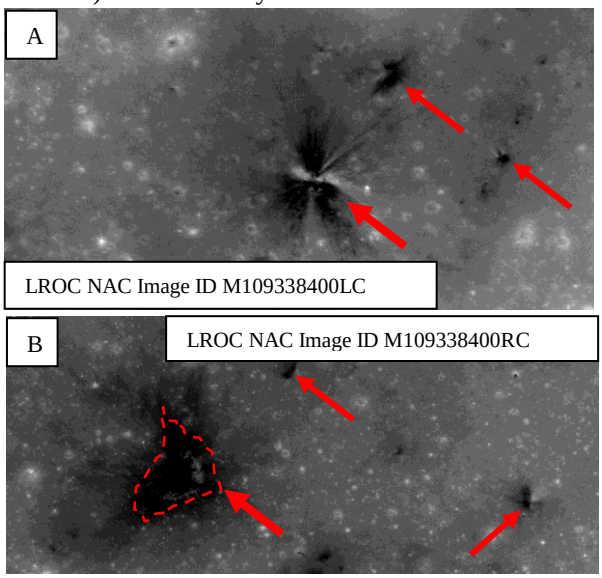

Fig. 4. A. Subset of LROC NAC Secne ID M109338400LC and B. LROC NAC Scene ID M109338400RC showing possible fissures/vents in the southern part of Sinus Aestuum I.

References: [1] Heiken G. H. et al. (1974) *GCA, 38,* 1703-1718. [2] Hawke B. R. et al. (1989) *Proceed. LPS XIX,* 255-268. [3] Weitz C. M. et al. (1998) *JGR, 103, E10,* 22,725-22,759. [4] Sunshine J. M. et al. (2010) *LPS XXXXI,* Abstract #1508. [5] Dhingra D. et al. (2011) *GRL, 38, L11201.* [6] Cloutis E. A. et al. (1986) *JGR, 91,* 11,641-11,653. [7] Raney R. K. et al. (2012) *JGR, 117,* E00H21. [8] Bhattacharya S. et al. (2012) *Curr. Sci. 103(01),* 21-23. [9] Cloutis E. A. et al. (2004) *Meteoritics & Planet. Sci., 39,* Nr 4. [10] Head J. W. et al. (2002) *JGR, 107,* E1.